Equilibrium Structure of *cis*-Hex-3-ene-1,5-diyne and Relevance to the Bergman Cyclization

Robert J. McMahon,*,† Robert J. Halter,† Ryan L. Fimmen,† Robb J. Wilson,‡,⊥ Sean A. Peebles,‡ Robert L. Kuczkowski,*,‡ and John F. Stanton*,§

Contribution from the Department of Chemistry, University of Wisconsin, Madison, Wisconsin 53706-1396, Department of Chemistry, University of Michigan, Ann Arbor, Michigan 48109-1055, and Department of Chemistry and Biochemistry, The University of Texas at Austin, Austin, Texas, 78712

Received September 27, 1999. Revised Manuscript Received November 16, 1999

Abstract: An accurate gas-phase structure determination of *cis*-hex-3-ene-1,5-diyne (**1**), the parent molecule for the Bergman cyclization reaction, has been achieved through a combination of Fourier transform microwave spectroscopy and computational quantum chemistry. The microwave spectra of seven isotopes of enediyne **1** have been observed using a pulsed-nozzle Fourier transform spectrometer. The ground-state rotational constants were corrected for vibrational effects and the equilibrium structure (R_e) was deduced. The equilibrium structure displays excellent agreement with that obtained from high-level ab initio calculations (CCSD(T)/cc-pVTZ). Both approaches confirm that the molecule has C_{2v} symmetry with slight deviations of the alkyne units (C−C≡C−H) from linearity. These groups distort away from each other in contra-distinction to their distortion during the Bergman cyclization reaction. The C1−C6 distance (4.32 Å), which has been viewed as a critical parameter governing reactivity in the Bergman cyclization, is notably longer than an earlier, widely publicized value (4.12 Å). An important role of the macrocyclic ring in enediyne antibiotics is to overcome an intrinsic distortion of the enediyne moiety in the direction *opposite* that of the reaction coordinate for Bergman cyclization.

Introduction

Cycloaromatization reactions, which convert a highly unsaturated acyclic molecule into a reactive diradical species containing an intact aromatic ring, represent fundamentally important transformations in organic chemistry.[1−5] Two important classes of cycloaromatization reactions involve the thermal cyclization of an enediyne (**1**) to a 1,4-didehydrobenzene (**2**; *p*-benzyne) (Bergman cyclization) and an eneyne allene (**3**) to an α,3-didehydrotoluene (**4**) (Myers-Saito cyclization) (Scheme 1). Spurred by the discovery that these two reactions constitute the basis for the biological activity of potent antitumor antibiotics,[2−7] cycloaromatization reactions have been the subject of tremendous interest since the late 1980s. Quite apart from a biological context, cycloaromatization reactions may also play a key role in the formation of aromatic compounds, fullerenes, carbon nanotubes, and soot during combustion.[8−10]

cis-Hex-3-ene-1,5-diyne (**1**)[11] represents the parent molecule for the Bergman cyclization.[12] Mechanistically, enediyne **1** represents a logical link between the open-chain hydrocarbons that are known to exist in interstellar clouds and the aromatic compounds that are thought to exist in these clouds.[8−10,13,14] To provide insight into both the Bergman cyclization and the organic chemistry of interstellar clouds, we sought to determine the microwave rotational spectrum and the gas-phase molecular structure of enediyne **1**. In the current study, we combine the techniques of synthetic organic chemistry, molecular spectroscopy, and computational quantum chemistry to afford detailed insight into the structure and spectroscopy of this fundamentally important species.

Scheme 1

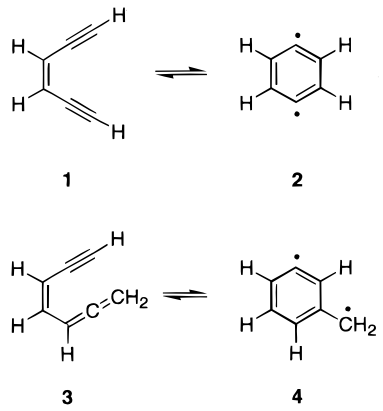

* To whom correspondence should be addressed.
† University of Wisconsin.
‡ University of Michigan.
§ University of Texas.
⊥ Present address: Department of Chemistry and Physics, Louisiana State University at Shreveport, Shreveport, LA 71115.

(1) Bergman, R. G. *Acc. Chem. Res.* **1973**, *6*, 25−31.
(2) Nicolaou, K. C.; Dai, W. M. *Angew. Chem., Int. Ed. Engl.* **1991**, *30*, 1387−1416.
(3) Nicolaou, K. C.; Smith, A. L. *Acc. Chem. Res.* **1992**, *25*, 497−503.
(4) Maier, M. E. *Synlett* **1995**, 13−26.
(5) Grissom, J. W.; Gunawardena, G. U.; Klingberg, D.; Huang, D. *Tetrahedron* **1996**, *52*, 6453−6518.
(6) Lee, M. D.; Ellestad, G. A.; Borders, D. B. *Acc. Chem. Res.* **1991**, *24*, 235−243.
(7) Goldberg, I. H. *Acc. Chem. Res.* **1991**, *24*, 191−198.
(8) Kroto, H. *Science* **1988**, *242*, 1139−1145.
(9) Hare, J. P.; Kroto, H. W. *Acc. Chem. Res.* **1992**, *25*, 106−112.
(10) Goroff, N. S. *Acc. Chem. Res.* **1996**, *29*, 77−83.
(11) Okamura, W. H.; Sondheimer, F. *J. Am. Chem. Soc.* **1967**, *89*, 5991−5992.
(12) Jones, R. R.; Bergman, R. G. *J. Am. Chem. Soc.* **1972**, *94*, 660−661.
(13) Kroto, H. W. *Int. J. Mass Spectrom. Ion Process.* **1994**, *138*, 1−15.
(14) Winnewisser, G.; Herbst, E. *Rep. Prog. Phys.* **1993**, *56*, 1209−1273.

10.1021/ja9934908 CCC: $19.00
Published on Web 01/19/2000

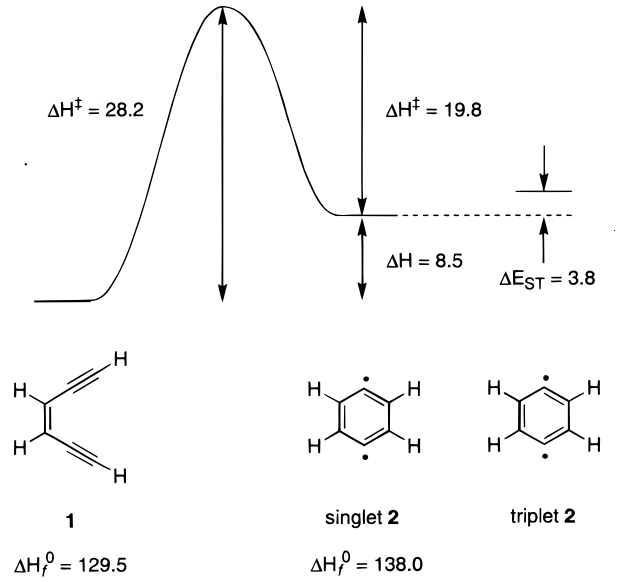

Figure 1. Potential energy diagram for Bergman cyclization of *cis*-hex-3-ene-1,5-diyne (**1**) to *p*-benzyne (**2**). Thermochemical data from ref 20; singlet−triplet splitting from ref 40.

Background

Bergman's classic studies of the thermal cycloaromatization of *cis*-hex-3-ene-1,5-diyne (**1**) to *p*-benzyne (**2**)[1,12] established an intellectual framework that unified earlier experimental observations concerning the chemistry of annulenes[15,16] and *p*-benzyne.[17−19] Sophisticated experimental and computational investigations now afford detailed insight into the potential energy surfaces for the Bergman (Figure 1)[20−32] and Myers-Saito[32−36] cyclizations as well as the structure and reactivity of 1,4-didehydrobenzene[37−49] and α,3-didehydrotoluene[50−52] diradicals. The enediyne-containing natural products calicheamicin, esperamicin, dynemicin, C-1027 chromophore, and kedarcidin utilize various fascinating "triggering" reactions to effect the Bergman cyclization under physiological conditions.[2−5] Similarly, neocarzinostatin chromophore effects the Myers-Saito cyclization. In both cases, the incipient diradical abstracts a hydrogen atom from each strand of the sugar phosphate backbone of DNA, leading ultimately to oxidative double-strand cleavage and cell death.

The ability of the enediyne natural products to effect thermal cycloaromatization reactions under physiological conditions stimulated tremendous interest in the structure−reactivity profile of the Bergman cyclization.[2−5] Considerable attention focused on the so-called "*c*−*d* distance" between the terminal carbons of the enediyne moiety. Nicolaou et al. noted that enediynes with *c*−*d* distances <3.20 Å cyclize spontaneously at 25 °C, while those with *c*−*d* distances >3.35 Å do not.[2,3] Although structural effects in the reactant, as reflected in the *c*−*d* distances, are undoubtedly significant,[53,54] it is widely appreciated that strain,[30,55−58] electronic factors,[30,58−61] and solvent effects[62] in the transition state must also be considered.

Results

Synthesis. Okamura and Sondheimer described the synthesis of the parent hex-3-ene-1,5-diyne (**1**) as a 40:60 mixture of cis: trans isomers,[11] a method later modified by Jones and Bergman to prepare deuterated isotopomers of **1**.[12] Subsequent developments in synthetic methodology now enable the selective preparation of either cis or trans isomer using transition-metal-catalyzed coupling reactions.[63] Pd-catalyzed coupling of *cis*-1,2-dichloroethylene and trimethylsilylacetylene afforded bis-(trimethylsilyl)enediyne (**5**) (Scheme 2).[64] Fluoride-induced

(15) Mayer, J.; Sondheimer, F. *J. Am. Chem. Soc.* **1966**, *88*, 603−604.
(16) Darby, N.; Kim, C. U.; Salaun, J. A.; Shelton, K. W.; Takada, S.; Masamune, S. *J. Chem. Soc., Chem. Commun.* **1971**, 1516−1517.
(17) Fisher, I. P.; Lossing, F. P. *J. Am. Chem. Soc.* **1963**, *85*, 1018−1019.
(18) Berry, R. S.; Clardy, J.; Schafer, M. E. *Tetrahedron Lett.* **1965**, 1003−1010.
(19) Hoyos de Rossi, R.; Bertorello, H. E.; Rossi, R. A. *J. Org. Chem.* **1970**, *35*, 3328−3332.
(20) Roth, W. R.; Hopf, H.; Horn, C. *Chem. Ber.* **1994**, *127*, 1765−1779.
(21) Roth, W. R.; Hopf, H.; Wasser, T.; Zimmermann, H.; Werner, C. *Liebigs Ann.* **1996**, 1691−1695.
(22) Koga, N.; Morokuma, K. *J. Am. Chem. Soc.* **1991**, *113*, 1907−1911.
(23) Kraka, E.; Cremer, D. *J. Am. Chem. Soc.* **1994**, *116*, 4929−4936.
(24) Lindh, R.; Persson, B. J. *J. Am. Chem. Soc.* **1994**, *116*, 4963−4969.
(25) Lindh, R.; Persson, B. J. *J. Am. Chem. Soc.* **1994**, *116*, 9411.
(26) Lindh, R.; Lee, T. J.; Bernhardsson, A.; Persson, B. J.; Karlstrom, G. *J. Am. Chem. Soc.* **1995**, *117*, 7186−7194.
(27) Lindh, R.; Ryde, U.; Schutz, M. *Theor. Chem. Acc.* **1997**, *97*, 203−210.
(28) Hoffner, J.; Schottelius, M. J.; Feichtinger, D.; Chen, P. *J. Am. Chem. Soc.* **1998**, *120*, 376−385.
(29) Chen, W. C.; Chang, N. Y.; Yu, C. H. *J. Phys. Chem. A* **1998**, *102*, 2584−2593.
(30) Schreiner, P. R. *J. Am. Chem. Soc.* **1998**, *120*, 4184−4190.
(31) Cramer, C. J. *J. Am. Chem. Soc.* **1998**, *120*, 6261−6269.
(32) Cramer, C. J.; Squires, R. R. *Org. Lett.* **1999**, *1*, 215−218.
(33) Myers, A. G.; Dragovich, P. S.; Kuo, E. Y. *J. Am. Chem. Soc.* **1992**, *114*, 9369−9386.
(34) Engels, B.; Hanrath, M. *J. Am. Chem. Soc.* **1998**, *120*, 6356−6361.
(35) Ferri, F.; Bruckner, R.; Herges, R. *New J. Chem.* **1998**, 531−545.
(36) Schreiner, P. R.; Prall, M. *J. Am. Chem. Soc.* **1999**, *121*, 8615−8627.
(37) Schottelius, M. J.; Chen, P. *J. Am. Chem. Soc.* **1996**, *118*, 4896−4903.
(38) Marquardt, R.; Balster, A.; Sander, W.; Kraka, E.; Cremer, D.; Radziszewski, J. G. *Angew. Chem., Int. Ed.* **1998**, *37*, 955−958.
(39) Kotting, C.; Sander, W.; Kammermeier, S.; Herges, R. *Eur. J. Org. Chem.* **1998**, 799−803.
(40) Wenthold, P. G.; Squires, R. R.; Lineberger, W. C. *J. Am. Chem. Soc.* **1998**, *120*, 5279−5290.
(41) Wenk, H. H.; Sander, W. *Eur. J. Org. Chem.* **1999**, 57−60.
(42) Sander, W. *Acc. Chem. Res.* **1999**, *32*, 669−676.
(43) Kraka, E.; Cremer, D. *Chem. Phys. Lett.* **1993**, *216*, 333−340.
(44) Kraka, E.; Cremer, D. *Chem. Phys. Lett.* **1994**, *219*, 160−160.
(45) Nicolaides, A.; Borden, W. T. *J. Am. Chem. Soc.* **1993**, *115*, 11951−11957.
(46) Logan, C. F.; Chen, P. *J. Am. Chem. Soc.* **1996**, *118*, 2113−2114.
(47) Cramer, C. J.; Nash, J. J.; Squires, R. R. *Chem. Phys. Lett.* **1997**, *277*, 311−320.
(48) Squires, R. R.; Cramer, C. J. *J. Phys. Chem. A* **1998**, *102*, 9072−9081.
(49) Cramer, C. J.; Debbert, S. *Chem. Phys. Lett.* **1998**, *287*, 320−326.
(50) Wenthold, P. G.; Squires, R. R. *J. Am. Chem. Soc.* **1994**, *116*, 6401−6412.
(51) Wenthold, P. G.; Wierschke, S. G.; Nash, J. J.; Squires, R. R. *J. Am. Chem. Soc.* **1994**, *116*, 7378−7392.
(52) Wenthold, P. G.; Wierschke, S. G.; Nash, J. J.; Squires, R. R. *J. Am. Chem. Soc.* **1994**, *116*, 4529.
(53) Konig, B.; Rutters, H. *Tetrahedron Lett.* **1994**, *35*, 3501−3504.
(54) Warner, B. P.; Millar, S. P.; Broene, R. D.; Buchwald, S. L. *Science* **1995**, *269*, 814−816.
(55) Snyder, J. P. *J. Am. Chem. Soc.* **1990**, *112*, 5367−5369.
(56) Magnus, P.; Fortt, S.; Pitterna, T.; Snyder, J. P. *J. Am. Chem. Soc.* **1990**, *112*, 4986−4987.
(57) Magnus, P.; Fairhurst, R. A. *J. Chem. Soc., Chem. Commun.* **1994**, 1541−1542.
(58) Schreiner, P. R. *J. Chem. Soc., Chem. Commun.* **1998**, 483−484.
(59) Schmittel, M.; Kiau, S. *Chem. Lett.* **1995**, 953−954.
(60) Kim, C.-S.; Russell, K. C. *J. Org. Chem.* **1998**, *63*, 8229−8234.
(61) Kaneko, T.; Takahashi, M.; Hirama, M. *Tetrahedron Lett.* **1999**, *40*, 2015−2018.
(62) Kim, C.-S.; Russell, K. C. *Tetrahedron Lett.* **1999**, *40*, 3835−3838.
(63) *Metal-Catalyzed Cross-Coupling Reactions*; Diederich, F., Stang, P. J., Eds.; Wiley-VCH Verlag: Weinheim, 1998.
(64) Chemin, D.; Linstrumelle, G. *Tetrahedron* **1994**, *50*, 5335−5344.

Scheme 2

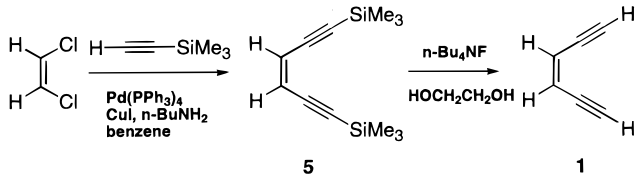

Scheme 3

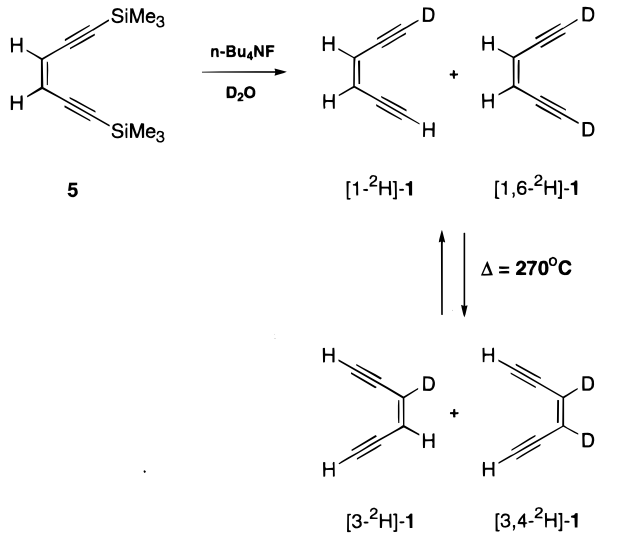

desilylation of the protected enediyne in a high boiling solvent allows the volatile enediyne **1** to be distilled from the reaction mixture as it is formed and collected in a liquid-nitrogen-cooled trap. The neat enediyne **1** decomposes slowly at −40 °C or rapidly at 25 °C. If the deprotection is performed in D_2O, a mixture of dideuterio [1,6-^{2}H], monodeuterio [1-^{2}H], and protio enediyne **1** is obtained (Scheme 3). This mixture was suitable for study by Fourier transform microwave rotational spectroscopy. A portion of this mixture was also used to generate additional deuterated isotopomers. The mixture was allowed to vaporize through a flash-vacuum pyrolysis tube (270 °C), thereby effecting deuterium scrambling via the reversible Bergman cyclization (Scheme 3). Collection of the product in a liquid-nitrogen-cooled trap afforded a mixture of dideuterio [1,6-^{2}H] and [3,4-^{2}H], monodeuterio [1-^{2}H] and [3-^{2}H], and protio enediyne **1**. This mixture was suitable for study by Fourier transform microwave rotational spectroscopy.

Even with the rotational spectra of four isotopomers of enediyne **1** in hand, the spectroscopic assignments for the [mono-^{13}C] isotopomers could not be assigned in natural abundance. Thus, it became necessary to synthesize a ^{13}C-enriched sample. We utilized trimethylsilyl-protected [1-^{13}C]-propynal, which was available from earlier studies in our group,[65,66] in a Wittig coupling reaction to afford a mixture of TMS-protected cis and trans enediynes (Scheme 4). The isomers were separated by column chromatography, and the trans isomer was subjected to photoequilibration conditions to afford more of the cis isomer. After deprotection in the usual manner, the [3-^{13}C] enediyne **1** was suitable for study by Fourier transform microwave rotational spectroscopy. With the additional spectroscopic data afforded by [3-^{13}C] enediyne **1**, the rotational spectra of the [1-^{13}C] and [2-^{13}C] isotopomers of enediyne **1** were detected in natural abundance.

(65) Seburg, R. A.; McMahon, R. J. *Angew. Chem., Int. Ed. Engl.* **1995**, *34*, 2009−2012.

(66) Seburg, R. A.; Patterson, E. V.; Stanton, J. F.; McMahon, R. J. *J. Am. Chem. Soc.* **1997**, *119*, 5847−5856.

Scheme 4

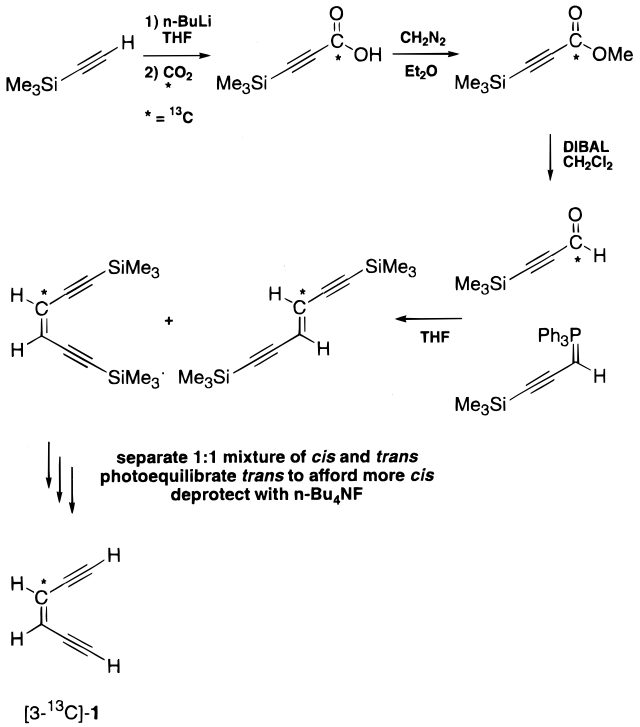

Table 1. Observed Rotational Transition Frequencies for *cis*-Hex-3-ene-1,5-diyne (**1**)

transition $J'K_a'K_c' - J''K_a''K_c''$	ν_{obs}/MHz	$\Delta\nu^a$/MHz
1 1 1 − 0 0 0	8 856.018	−0.002
1 1 0 − 1 0 1	5 054.558	0.002
2 1 2 − 1 0 1	12 657.520	−0.001
2 0 2 − 1 1 1	4 627.980	0.001
2 1 1 − 2 0 2	5 858.016	−0.001
2 2 0 − 2 1 1	13 083.733	−0.001
2 2 1 − 2 1 2	15 163.362	0.001
3 1 3 − 2 0 2	16 132.263	0.001
3 0 3 − 2 1 2	9 547.129	−0.000
3 1 2 − 3 0 3	7 207.759	−0.004
3 2 1 − 3 1 2	12 381.531	0.000
3 2 2 − 3 1 3	16 293.760	0.002
4 0 4 − 3 1 3	14 430.767	−0.002
4 1 3 − 4 0 4	9 232.962	0.004
4 1 3 − 3 2 2	7 369.970	0.001
4 2 2 − 4 1 3	11 828.288	−0.001
4 2 3 − 4 1 4	17 819.864	0.000
5 1 4 − 5 0 5	12 009.159	−0.003
5 1 4 − 4 2 3	13 330.400	0.001
5 2 3 − 5 1 4	11 668.885	−0.001
6 1 5 − 6 0 6	15 494.462	0.001
6 2 4 − 6 1 5	12 107.111	0.002
7 2 5 − 7 1 6	13 294.784	−0.001

[a] $\Delta\nu = \nu_{obs} - \nu_{calc}$; ν_{calc} obtained with the corresponding constants in Table 2.

Rotational Spectra. Enediyne **1** exhibits a pure *b*-type spectrum, as expected for this planar species with C_{2v} symmetry. The assignments of spectra were guided by spectral predictions and Stark effect experiments on selected transitions. See Table 1 for a list of observed frequencies for the normal isotopic species. Frequencies for the other isotopic species are available as Supporting Information. The frequencies were fit with an S-reduced Watson Hamiltonian (I^r representation).[67] The fitted

Table 2. Spectroscopic Fitted Constants for Isotopomers of *cis*-Hex-3-ene-1,5-diyne (**1**)[a]

	normal	[1-^{2}H]	[1,6-^{2}H]	[3,4-^{2}H]	[3-^{13}C]	[2-^{13}C]	[1-^{13}C]
$A_0^{(S)}$ (MHz)	6955.2978(8)	6639.009(4)	6322.155(5)	6243.388(3)	6840.548(4)	6954.618(3)	6854.856(4)
$B_0^{(S)}$ (MHz)	2621.5146(3)	2519.848(2)	2428.664(2)	2580.377(2)	2615.396(2)	2592.949(2)	2559.612(2)
$C_0^{(S)}$ (MHz)	1900.7330(3)	1823.533(1)	1751.713(2)	1822.884(1)	1888.849(1)	1885.624(1)	1860.615(2)
D_J (kHz)	2.968(9)	2.86(5)	2.66(5)	2.91(8)	3.07(4)	2.83(5)	2.99(8)
D_{JK} (kHz)	−19.80(4)	−18.4(2)	−18.0(2)	−14.9(6)	−18.8(3)	−19.1(2)	−18.4(2)
D_K (kHz)	43.3(1)	38.1(9)	36.9(1.2)	34.0(7)	41.4(8)	43.2(7)	41.9(9)
d_1 (kHz)	−1.168(2)	−1.09(1)	−1.04(1)	−1.68(13)	−1.12(2)	−1.118(8)	−1.228(9)
d_2 (kHz)	−0.0645(9)	−0.066(6)	−0.066(4)	−1.46(14)	0.013(7)	−0.03(1)	0.003(5)
n[b]	23	21	17	12	18	19	20
$\Delta\nu_{rms}$ (kHz)[c]	1.9	8.8	9.4	4.7	8.1	6.8	9.7
P_{aa} (amu Å^2)[d]	193.005	200.791	208.328	196.077	193.456	195.127	197.670
P_{bb} (amu Å^2)	72.883	76.353	80.179	81.167	74.103	72.890	73.951
P_{cc} (amu Å^2)	−0.222	−0.231	−0.241	−0.220	−0.224	−0.222	−0.225
det. constants[e]							
A_0'' (MHz)	6955.3034(9)	6639.014(4)	6322.160(5)	6243.385(3)	6840.554(4)	6954.623(3)	6854.859(2)
B_0'' (MHz)	2621.4982(4)	2519.833(2)	2428.649(2)	2580.359(2)	2615.382(2)	2592.933(2)	2559.594(1)
C_0'' (MHz)	1900.7212(3)	1823.522(2)	1751.703(2)	1822.872(1)	1888.839(2)	1885.613(1)	1860.606(1)

[a] Uncertainty estimates are 1 standard deviation. [b] Number of transitions in the fit. [c] $\Delta\nu = \nu_{obs} - \nu_{calc}$. [d] $P_{aa} = 0.5(I_b + I_c - I_a) = \Sigma m_i a_i^2$; P_{bb}, P_{cc} similarly. [e] These are the Watson determinable rotational constants for each isotope which are independent of the Hamiltonian reduction method.[67]

Table 3. Stark Coefficients and Dipole Moment[a]

transition	|M|	$(\Delta\nu/\epsilon^2)$ (obs) MHz/(kV/cm)^2	(obs − calc) MHz/(kV/cm)^2
$1_{11}-0_{00}$	0	0.383(5)	−0.025
$2_{12}-1_{01}$	0	0.124(12)	−0.002
	1	0.460(12)	−0.007
$3_{21}-3_{12}$	1	0.529(12)	0.019
	2	0.390(9)	0.005
	3	0.192(10)	0.014
	$\|\mu_b\| = \|\mu_T\| = 0.18(1)$ D		

[a] Uncertainty estimates are 1 standard deviation.

rotational constants ($A_0^{(S)}$ etc.) and other spectroscopic parameters are given in Table 2.

To characterize the structural parameters of the enediyne with minimal assumption, spectra were observed for each of the singly substituted ^{13}C species, the mono- and di-substituted deuterium species on the alkyne carbons, and the di-substituted deuterium species on the alkene carbons. (A minimum of five unique isotopomers is necessary for a complete structural analysis of this molecule.) Only *b*-type *R*- and *Q*-branch transitions were assigned for all species. There was no observed quadrupole splitting in the deuterated spectra, and line broadening was minimal. The carbons are numbered as follows: the terminal alkyne carbons are labeled C1 and C6, and the others are numbered seriatim C2 and C5 (inner alkyne) and C3 and C4 (alkene). The deuterated and the [3-^{13}C] species were observed in enriched samples. The other two carbon isotopes were observed in natural abundance. The strongest [1-^{13}C] and [2-^{13}C] transitions could be observed in about 100 gas pulses; about 16 000 spectra were averaged to obtain good frequency determinations for average-strength transitions.

Dipole Moment. The second-order Stark effects of six *M* components of three rotational transitions of the normal isotopic species were measured. The Stark coefficients ($\Delta\nu/\epsilon^2$) were fit using perturbation coefficients calculated from the spectroscopic constants to give $|\mu_b| = |\mu_T| = 0.18(1)$ D (Table 3).

Structure. As suggested by numerous computational studies,[23,26,29−31,68] enediyne **1** is expected to be a symmetric planar molecule. The *b*-type transitions and small inertial defect (defined below) are consistent with such a structure. The questions to be answered lie in the particulars of the bond lengths and angles.

Normally, each of the three rotational constants of each isotopomer contributes to the structural determination, but for a planar molecule only two are independent, since $I_a + I_b = I_c$ for a rigid system. For enediyne **1**, there are five unique bond lengths and four unique angles. Therefore, four isotopomers, in addition to the normal species, are required for a complete structural determination. In the calculation of the structure, the molecule was constrained to have two perpendicular planes of symmetry, one in the plane of the molecule and one perpendicular to the alkene σ bond (C_{2v}). Spectra of seven isotopes were obtained, giving an overdetermined data set of 14 independent equations for the structural determination.[69] Since each atom has been isotopically substituted at least once, the inertial equations are free of linear dependencies and indeterminacy problems that sometimes can arise with minimal data sets.

A common characteristic of planar molecules is a quantity known as the inertial defect, which is represented by $I_c - I_b - I_a = \Delta$. A rigid planar molecule would have $\Delta = 0$. However, the use of ground-state moments of inertia which contain zero-point vibrational effects leads to small positive values for planar molecules which complicate a structural determination. For enediyne **1**, the inertial defect is $\Delta = 0.444$ amu Å^2 (Table 2).

Structures calculated from the moments of inertia, uncorrected for zero-point vibrational effects, are listed in Table 4 as the R_0 and R_s structures 1−3. The R_0 structures, the so-called effective structures,[67] were derived by least-squares fitting either the 14 I_a and I_b moments of inertia or all 21 *I*'s. The fits of the 14 *I*'s appeared to be very good ($\Delta I_{rms} = 0.0020$ amu Å^2) while the fit of 21 *I*'s was degraded to a $\Delta I_{rms} = 0.1998$ amu Å^2 because of the residual inertial defect. The R_s structure, that is, the so-called substitution structure,[67] was derived by calculating coordinates separately for each atom using isotopic substitution equations first derived by Kraitchman.[67,70] Since vibration−rotation effects partially cancel when taking differences in moments of inertia in this procedure, the R_s structure is often

(67) Gordy, W.; Cook, R. L. *Microwave Molecular Spectra*, 3rd ed.; Wiley-Interscience: New York, 1984.

(68) *The Challenge of d and f Electrons: Theory and Computation*; Salahub, D. R., Zerner, M. C., Eds.; American Chemical Society: Washington, DC, 1989.

(69) The [1-^{2}H] and [1,6-^{2}H] species are not rigorously independent data sets if C_{2v} symmetry is imposed.

(70) Kraitchman, J. *Am. J. Phys.* **1953**, *21*, 17−24.

Table 4. Structural Parameters for *cis*-Hex-3-ene-1,5-diyne (**1**)

	structure[a]							
parameter	1 R_0	2 R_0	3 R_s	4 R_e	5 R_e	6 R_e	7 R_s	8 R_s
C═C (Å)	1.345	1.346	1.345	1.350	1.348	1.347	1.348	1.348
C−C (Å)	1.420	1.421	1.435	1.419	1.421	1.421	1.418	1.418
C≡C (Å)	1.212	1.213	1.198	1.208	1.208	1.208	1.210	1.210
═C−H (Å)	1.099	1.097	1.099	1.080	1.078	1.080	1.079	1.079
≡C−H (Å)	1.054	1.055	1.057	1.059	1.061	1.062	1.061	1.061
C═C−C (deg)	123.9	123.9	123.5	123.9	124.0	123.9	124.0	124.0
C−C≡C (deg)	178.9	179.0	178.0	178.8	178.9	178.8	178.9	178.9
C≡C−H (deg)	179.5	179.6	178.9	179.3	179.3	179.4	179.4	179.4
C═C−H (deg)	120.9	120.9	120.8	118.3	118.2	118.6	118.6	118.6
ΔI_{rms} (amu Å^2)[b]	0.002	0.200		0.043	0.005	0.006		

[a] R_0 effective structures 1 and 2 were obtained by least-squares fitting the 14 I_a, I_b, or 21 I_a, I_b, I_c determinable moments from Table 2, respectively. R_s substitution structure 3 was obtained from Kraitchman's equations which determine atom coordinates from differences in moments of inertia upon isotopic substitution using the determinable constants, Table 2. R_e equilibrium structures 4−6 were obtained by fitting the 21 rotational constants in Table 6 to empirical equilibrium rotational constants obtained using Force Fields I−III, respectively. R_s substitution structures 7−8 were obtained from Kraitchman's equations using the equilibrium constants in Table 6 (structure 7, FF II; structure 8, FF III). [b] $\Delta I = [I_{x(obs)} - I_{x(calc)}]$ where I_x is one of the three principal moments of inertia.

Table 5. Principal Axis Coordinates of *cis*-Hex-3-ene-1,5-diyne (**1**)

	fit to 14 moments[a]		Kraitchman[b]	
	a/Å	*b*/Å	*a*/Å	*b*/Å
$C_{1,6}$	0.6723	−1.1126	0.6724	1.1122
$C_{2,5}$	1.4649	0.0657	1.4643	0.0838
$C_{3,4}$	2.1605	1.0577	2.1608	1.0582
$H_{1,6}$	1.2360	−2.0557	1.2354	2.0554
$H_{3,4}$	2.7578	1.9266	2.7594	1.9290

[a] Obtained by least-squares fitting of the 14 I_a and I_b moments of inertia based on the spectroscopic determinable constants in Table 2. The *c* coordinate is assumed to be zero. Atoms C4, C5, C6, H4, and H6 have negative signs for *a*. [b] Calculated with Kraitchman's equations[67,70] from differences in the spectroscopic determinable moments upon isotopic substitution. Only the absolute value is determined. Kraitchman coordinate values near zero have a higher uncertainty, as in the *b* coordinate for C2.

considered the best approximation to the equilibrium structure that can be obtained from ground-state spectroscopic moments of inertia otherwise uncorrected for vibrational effects. Table 5 lists the principal axis coordinates for both the R_0 and the R_s structures 1 and 3.

It was apparent that these three structures showed significant variation among themselves and with the several high level ab initio structures already in the literature. This motivated us to undertake correcting the ground-state rotational constants for zero-point vibrational effects. We used the equation

$$A_0 = A_e - \Sigma_i \alpha_i^A/2$$

where A_0 is the ground-state rotational constant, A_e is the equilibrium value, and α_i^A are the vibration−rotation interaction constants which are a function of the vibrational force field. Analogous equations hold for B_0 and C_0. The rotational constants are inversely proportional to the moments of inertia via I_a (amu Å^2) = 5.05379 × 10^5(*A*)$^{-1}$ (MHz).

Pioneering studies of anharmonic force constant calculations by Allen et al.[71,72] clearly demonstrated that vibrational corrections to rotational constants are usually predicted relatively accurately at the self-consistent field (SCF) level of theory. Although sophisticated treatments of electron correlation and large basis sets have recently been used to calculate very accurate vibrational corrections to rotational constants for molecules containing up to about six atoms,[73−75] such an approach would be extremely expensive for enediyne **1**. Hence, we have chosen to determine vibrational corrections by means of three approaches. In the first (hereafter called I), both the quadratic and cubic force fields of **1** were calculated at the SCF level using the DZP basis set[76] and the corresponding equilibrium geometry. The second approach (II) is based on quadratic force constants and an equilibrium structure determined with the same basis set, but with inclusion of electron correlation approximated by partial fourth-order many-body perturbation theory (SDQ-MBPT(4)). The cubic force constants were then determined at the SCF level at the same geometry and transformed into the normal coordinate representation defined by the SDQ-MBPT(4) harmonic force field. The third approach is identical to II, except that the TZ2P basis was used instead of the DZP set.

The ab initio force fields determined by approaches I−III were used to calculate complete sets of rotation−vibration interaction constants for the seven isotopomers, and a set of empirical equilibrium rotational constants (A_e, B_e, C_e) was obtained for each by correcting Watson's determinable parameters[67] A_0'', B_0'', and C_0'' for both vibrational and centrifugal distortion effects. Following this, "experimental" equilibrium structures were obtained by least-squares refinement of the structural parameters so as to provide the best fit to the 21 empirical A_e, B_e, and C_e constants. The structures obtained from this procedure are documented in Table 4, structures 4−6, while the corrections $A_0'' - A_e$, $B_0'' - B_e$, and $C_0'' - C_e$ and corresponding equilibrium rotational constants for each isotopomer can be found in Table 6.

The magnitude of the inertial defect ($I_c^e - I_b^e - I_a^e$) is reduced with respect to the relatively large value of 0.444 amu Å^2 associated with the ground-state rotational constants in all three sets of empirical equilibrium rotational constants. Inertial defects associated with rotational constants based on force field I are generally lower by a factor of 4 (the maximum value of Δ is

(71) Allen, W. D.; Yamaguchi, Y.; Csaszar, A. G.; Clabo, D. A.; Remington, R. B.; Schaefer, H. F. *Chem. Phys.* **1990**, *145*, 427−466.
(72) Clabo, D. A.; Allen, W. D.; Remington, R. B.; Yamaguchi, Y.; Schaefer, H. F. *Chem. Phys.* **1988**, *123*, 187−239.
(73) Botschwina, P.; Horn, M.; Seeger, S.; Flugge, J. *Chem. Phys. Lett.* **1992**, *195*, 427−434.
(74) McCarthy, M. C.; Gottlieb, C. A.; Thaddeus, P.; Horn, M.; Botschwina, P. *J. Chem. Phys.* **1995**, *103*, 7820−7827.
(75) Stanton, J. F.; Lopreore, C. L.; Gauss, J. *J. Chem. Phys.* **1998**, *108*, 7190−7196.
(76) Redmon, L. T.; Purvis, G. D.; Bartlett, R. J. *J. Am. Chem. Soc.* **1979**, *101*, 2856−2862.

Table 6. Empirical Equilibrium Rotational Constants (MHz) for *cis*-Hex-3-ene-1,5-diyne (**1**) and Isotopomers

A_e	B_e	C_e	$A_0'' - A_e$	$B_0'' - B_e$	$C_0'' - C_e$
		Force Field I SCF/DZP			
6974.295	2617.014	1902.252	−18.99	4.48	−1.53
6655.777	2515.393	1824.823	−16.76	4.44	−1.30
6336.882	2424.240	1752.801	−14.72	4.41	−1.10
6255.324	2579.081	1825.625	−11.94	1.28	−2.75
6859.111	2610.871	1890.361	−18.56	4.51	−1.52
6973.851	2588.459	1887.084	−19.23	4.47	−1.47
6873.674	2555.193	1862.053	−18.82	4.40	−1.45
		Force Field II SDQ-MBPT(4)/DZP			
6967.737	2618.430	1903.134	−12.43	3.07	−2.41
6649.093	2516.704	1825.601	−10.08	3.13	−2.08
6330.036	2425.484	1753.493	−7.88	3.17	−1.79
6249.941	2580.802	1826.527	−6.56	−0.44	−3.66
6852.657	2612.290	1891.231	−12.10	3.09	−2.39
6967.409	2589.806	1887.940	−12.79	3.13	−2.33
6867.271	2556.576	1862.924	−12.41	3.02	−2.32
		Force Field III SDQ-MBPT(4)/TZ2P			
6963.940	2623.050	1905.238	−8.64	−1.55	−4.52
6645.710	2521.028	1827.573	−6.70	−1.19	−4.05
6326.995	2429.554	1755.344	−4.84	−0.91	−3.64
6247.859	2584.776	1828.268	−4.47	−4.42	−5.40
6848.872	2616.873	1893.292	−8.32	−1.49	−4.45
6963.563	2594.389	1890.043	−8.94	−1.46	−4.43
6863.579	2561.060	1864.983	−8.72	−1.47	−4.38

0.105 amu Å^2, 0.098 amu Å^2 for the normal isotopomer). A dramatic improvement is noted when the SDQ-MBPT(4) harmonic force fields are used; the largest Δ is reduced to 0.012 and 0.019 amu Å^2 for force fields II and III, respectively. For the normal isotopomer, a roughly 40-fold improvement is achieved relative to the value obtained from the uncorrected ground-state rotational constants. Nevertheless, equilibrium structures derived from empirical A_e, B_e, and C_e values based on force fields I, II, and III are very similar. For bond distances, the largest variance is found for the nominal C−C double bond (1.350 Å with set I; 1.347 Å with set III), while the C═C−H bond angle varies by 0.4°.

It is difficult to estimate the uncertainty in the derived equilibrium structural parameters documented in Tables 4 and 7. However, a previous study of dioxirane that compared structures calculated in the manner described here using both SCF (similar to I of the present work) and highly correlated force fields gave distances and angles that differed on the order of 0.001 Å and 0.1°.[75] Effects of similar magnitude are found for the C−H bond distance in methane.[77] In view of the greater rigidity of those systems relative to enediyne **1**, however, a more conservative estimate of the accuracy is appropriate. Judging from the variation of parameters obtained from the three refinement procedures based on force fields I, II, and III, and the agreement between these structural parameters and those obtained in the most sophisticated ab initio calculations (vide infra), we believe that bond distances and angles inferred from force field III have uncertainties of no more than 0.003 Å and 0.5°, respectively. These parameters are considered the best estimates of the equilibrium structural parameters and can be used as a reference point for comparison with various ab initio calculations.

We list in Table 7 the ab initio structures that were determined in the course of this study: SCF/TZ2P, CCSD/TZ2P, CCSD(T)/TZ2P, and CCSD(T)/cc-pVTZ. For comparison, we also list several other ab initio and density functional theory calculations from the literature. It is clear that the highest level ab initio and experimental equilibrium structures are in excellent agreement.

(77) Stanton, J. F., unpublished results.

Discussion

A detailed understanding of the structure and spectroscopy of enediyne **1** affords insight into a diverse range of topics. Various aspects of this study are worthy of note. Comments will be directed on the relationship of the structure to enediyne chemistry, structural-vibrational effects discernible from the synergism between the experimental and ab initio approaches, empirical comparisons with some other related species, and bond alternation effects in theoretical calculations.

Enediyne Chemistry. This study establishes unequivocally that a small distortion from linearity occurs in the alkyne groups in a direction *counter* to incipient Bergman cyclization. Both the C−C≡C angle (178.8°) and the C≡C−H angle (179.4°) deviate from linearity in the direction *opposite* to the reaction coordinate for thermal cycloaromatization (Table 7, Figure 2). Although these deviations are small, it is important to keep in mind that the hypothetical symmetric structure with linear alkyne units is not a stationary point on the potential energy surface (determined by symmetry). This means, for example, that structures containing a linear C−C≡C or C≡C−H unit are *not* transition states for bending vibrations about a symmetrical (linear) structure. Indeed, both our experimental data and our calculations show that the *equilibrium* structure for the alkyne units of enediyne **1** is bent. In this sense, the ability to measure the deviation of an angle at an sp carbon center from 180° is no different than the ability to measure the deviation of an angle at an sp^2 carbon center from 120°. Although previous computational studies inevitably predicted the occurrence of these distortions, the data were largely presented without comment. Moreover, discrepancies and incomplete information regarding both the magnitude and direction of these deviations left considerable doubt concerning the reliability of computational methods to assess these subtle structural effects.[23−26,28−32] Critical reassessment of the literature (including data contained in Supporting Information), new information concerning previously published results,[78] and our own computational studies enable us to conclude that a wide variety of theoretical treatments afford consistent predictions concerning the direction of distortion for the alkyne units of enediyne **1**.

Distortions of this type are precedented in systems with two triple bonds in close proximity. A repelling of the alkyne groups was recognized in $CH_2(C{\equiv}CH)_2$ and related species in an earlier investigation by the Michigan authors.[79] Although detailed structural comparisons with the isomeric *trans*-hex-3-ene-1,5-diyne would be highly desirable, the inversion symmetry of the trans isomer ($\mu = 0$) precludes investigation by microwave spectroscopy. Photoelectron spectroscopy of *cis*- and *trans*-hex-3-ene-1,5-diyne reveals the destabilization of the in-plane π-orbital of the cis isomer by a combination of through-space and through-σ-bond interactions.[80]

(78) Cremer, D., personal communication. In Figure 1 of ref 23, the CCSD(T) value for the C═C−C angle should be 124.1° instead of 120.6°, and the values for the C−C≡C angles should be 182° instead of 178°, thereby indicating a distortion in the opposite direction of that implied in the figure.

(79) Kuczkowski, R. L.; Lovas, F. J.; Suenram, R. D.; Lattimer, R. P.; Hillig, K. W.; Ashe, A. J. *J. Mol. Struct.* **1981**, *72*, 143−152.

(80) Brogli, F.; Heilbronner, E.; Wirz, J.; Kloster-Jensen, E.; Bergman, R. G.; Vollhardt, K. P. C.; Ashe, A. J. *Helv. Chim. Acta* **1975**, *58*, 2620−2645.

Table 7. Equilibrium Structural Parameters for *cis*-Hex-3-ene-1,5-diyne (**1**) and Comparison to Various Theoretical Structures

						literature				
parameter	equilibrium R_e[a]	CCSD(T)/ cc-pVTZ	CCSD(T)/ TZ2P	CCSD/ TZ2P	SCF/ TZ2P	CCSD(T)/ 6-31G(d,p)[b]	CAS(12,12)/ TZ2P[c]	CAS(6,6)/ 3-21G[d]	BLYP/ 6-31G*[e]	BPW91/ cc-pVDZ[f]
C═C (Å)	1.347	1.347	1.352	1.342	1.324	1.357	1.361	1.337	1.370	1.369
C−C (Å)	1.421	1.420	1.430	1.431	1.432	1.431	1.432	1.426	1.418	1.417
C≡C (Å)	1.208	1.206	1.207	1.205	1.183	1.220	1.204	1.200	1.223	1.227
═C−H (Å)	1.080	1.079	1.081	1.080	1.072	1.084	1.072	1.072	1.096	1.102
≡C−H (Å)	1.062	1.059	1.063	1.061	1.054	1.064	1.053	1.051	1.072	1.078
C1−C6 (Å)	4.321	4.365	4.358	4.365	4.402	4.412	4.433	4.339	4.541	4.548
C═C−C (deg)	123.9	124.3	124.0	124.3	125.2	124.1[g]	124.9[h]	124.3	125.7	125.6
C−C≡C (deg)	178.8	178.5	178.6	178.8	178.0	178.0	179.3[i]	178.8	177.2	177.4
C≡C−H (deg)	179.4	179.0	179.1	179.1	179.3	178.4	179.0	179.6	178.2	178.7
C═C−H (deg)	118.6	118.7	118.8	118.9	118.7	118.8	118.3	119.1	117.6	117.8

[a] Structure 6, Table 4. Uncertainties are 0.003 Å in distances and 0.5° in angles; see text. [b] Reference 23. [c] Reference 26. [d] Reference 28. [e] Reference 30. [f] Reference 31. [g] Reference 78. [h] Value not reported in paper. It was calculated from the reported compliments of that angle around the carbon. [i] 360.0°−180.7° where the latter is reported in the paper. The tabulated value is given to be consistent with the angle definitions used in the other columns.

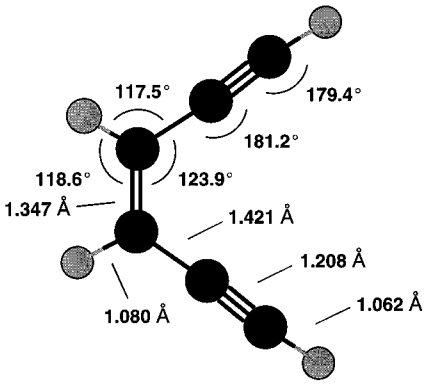

Figure 2. Equilibrium structure (R_e) of *cis*-hex-3-ene-1,5-diyne (**1**).

Stimulated by the intense interest in the structure−property relationships of macrocyclic enediyne antibiotics, considerable attention has focused on the relationship between the *c*−*d* distance (C1−C6 distance in enediyne **1**) and the rate of Bergman cyclization.[2−5] The *c*−*d* distance for the parent enediyne **1** represents an important benchmark in these comparisons. A *c*−*d* distance of 4.12 Å, obtained by MM2 calculations,[81] has received widespread attention because of the significant impact of Nicolaou's review articles.[2,3] Our experimental results establish the *c*−*d* equilibrium distance in enediyne **1** as 4.32 Å (Table 7), thereby demonstrating that the earlier value was significantly underestimated. This larger distance is determined not so much by the subtle distortions of the alkyne units from linearity as by the C═C−C bond angle (123.9°). In contrast to the MM2 calculation, previous ab initio and density functional theory calculations overestimate the *c*−*d* equilibrium distance by 0.1−0.2 Å (Table 7). The structural data for enediyne **1** thus provide an interesting context for assessing the Bergman cyclization of enediyne antibiotics: the macrocyclic ring serves to aid the enediyne moiety to overcome an intrinsic distortion in the direction *opposite* that of the cycloaromatization reaction coordinate. This structural effect does not necessarily imply a significant consequence in terms of energy; in enediyne **1**, the vibrational normal mode that becomes the reaction coordinate for cyclization is calculated to occur at low frequency (a_1, 103 cm^{-1}; in-plane scissoring of alkyne units; SDQ/TZ2P level of theory).

With the rotational spectrum of enediyne **1** now in hand, experiments in molecular spectroscopy offer the possibility of important new insights into problems in astronomy and combustion. By subjecting simple organic species such as acetylene and diacetylene to a pulsed DC electrical discharge, Thaddeus, Gottlieb, McCarthy, and their collaborators have generated and characterized a wide variety of reactive organic species by rotational spectroscopy.[82,83] Remarkably, many of these reactive species have been subsequently detected as constituents of interstellar clouds by microwave radioastronomy. The laboratory detection of enediyne **1** in an electric discharge of this type would carry important implications concerning the chemistry of interstellar clouds. Our rotational spectrum also enables a radioastronomical search for enediyne **1**. The detection of an interstellar molecule depends on the intensity of the rotational emission spectrum, which is related to both molecular abundance and the inherent intensity of the microwave rotational transitions.[14,82] Molecules occurring in low abundance (e.g., the cumulene carbene H_2C_6) may be detected if their rotational transitions are very strong (i.e., if the molecule has a large dipole moment).[84] Conversely, molecules with weak rotational transitions (e.g., CO, $\mu = 0.1$ D) may be detected if they occur in sufficiently high abundance.[14] The small dipole moment of enediyne **1** ($\mu = 0.18$ D; Table 3) implies that this molecule will not be detected unless it occurs in relatively high abundance. The polar mono- and di-nitrile analogues of enediyne **1** represent more realistic targets for astronomical detection, and efforts in this direction are currently underway.

Structural-Vibrational Effects. The spectroscopic analysis uncorrected for vibrational effects shows a variation in the derived parameters dependent on the procedure used to calculate them. While these are small on an absolute scale (≈0.015 Å, 1°), they were sufficiently large to frustrate the search for the ^{13}C isotopic species in natural abundance until after the enriched deuterated and [3-^{13}C] species were assigned. The significant deviation of several heavy atom R_s parameters from the equilibrium values, contrary to the usual expectation, is also notable. This arises from the high sensitivity of the small *b* coordinate for C2 to residual vibrational effects which do not precisely cancel in the Kraitchman substitution calculation. Vibrational effects on the rotational constants, which change in a complex manner upon isotopic substitution, are the origin of these discrepancies. It is possible to correct the ground-state

(81) Nicolaou, K. C.; Zuccarello, G.; Ogawa, Y.; Schweiger, E. J.; Kumazawa, T. *J. Am. Chem. Soc.* **1988**, *110*, 4866−4868.

(82) Thaddeus, P.; Gottlieb, C. A.; Mollaaghababa, R.; Vrtilek, J. M. *J. Chem. Soc., Faraday Trans.* **1993**, *89*, 2125−2129.

(83) McCarthy, M. C.; Travers, M. J.; Kovacs, A.; Gottlieb, C. A.; Thaddeus, P. *Astrophys. J. Suppl. Ser.* **1997**, *113*, 105−120.

(84) McCarthy, M. C.; Travers, M. J.; Kovacs, A.; Chen, W.; Novick, S. E.; Gottlieb, C. A.; Thaddeus, P. *Science* **1997**, *275*, 518−520.

Table 8. Selected Values of Bond Distances (in Å)

species	formula	structure[a]	C≡C	C═C	C−C	ref
enediyne **1**	C_6H_4	R_e	1.208(3)	1.347(3)	1.421(3)	*b*
phenyl acetylene	C_6H_5CCH	R_s, R_0	1.208(2)	1.39(1)	1.448(10)	*c*
1,4-pentadiyne	C_5H_4	R_0	1.206(10)		1.471(10)	*d*
methyl acetylene	CH_3CCH	R_e	1.204(1)		1.458(2)	*e*
acetylene	HCCH	R_e	1.203(2)			*c*
diacetylene	HCCCCH	R_0			1.376	*c*
benzene	C_6H_6	R_0		1.396(5)		*c*
ethylene	C_2H_4	R_e		1.334(2)		*f*
propene	CH_2CHCH_3	R_e		1.334(1)	1.496(1)	*g*
ethane	C_2H_6	R_e			1.522(2)	*g*

[a] Equilibrium parameters (R_e); ground-state effective parameters (R_0); Kraitchman substitution parameters (R_s). [b] This work. [c] Reference 119. [d] Reference 79. [e] Reference 95. [f] Reference 120. [g] Reference 121.

constants using ab initio calculations which provide the second and third derivatives of the energy that are required to evaluate vibrational and centrifugal contributions which can be subtracted from the measured rotational constants to yield empirical equilibrium values A_e, B_e, and C_e. The relative insensitivity of the corrected constants and resultant structure to the level of calculation makes it attractive to combine this more regularly with experimental results. This then provides experimental equilibrium structures for comparison with other structures and calculations.

Regarding a specific comparison of the theoretical and experimental R_e values, several parameters are consistently troublesome. Clearly, several hydrogen-related R_0, R_s parameters are overestimated without corrections for vibrational effects. The calculated carbon−carbon distances are also variable over a range of about 0.01 Å, depending on the ab initio method.

Empirical Comparisons. This study shows that differences of ≈0.01 Å and 1°−2° from spectroscopic studies of small hydrocarbons may not be unambiguously established unless vibrational effects in the derived moments of inertia are minimized. With this caveat notwithstanding, a few comments are appropriate on corresponding distances in other conjugated molecules. Table 8 provides a number of comparisons of carbon−carbon bond lengths of the enediyne with the corresponding distances of other conjugated molecules. Two points are apparent. First, the carbon−carbon single-bond distance is very short and approaches the value in diacetylene. This conjugation effect is somewhat less in phenylacetylene (1.45 Å). Some of this shortening arises from well-known differences in hybridization effects on carbon. Other spectroscopic and ab initio studies also discuss conjugation effects on bond length.[80,85] These shortening effects from multiple conjugation are much less apparent in the alkene linkage and effectively absent in the alkyne bonds. In fact, the double bond in ethylene is about 0.01 Å shorter than that in the enediyne.

Subtle distortions of acetylene and nitrile groups from linearity, such as those observed for enediyne **1** (Figure 2), have been observed previously for vinyl acetylene,[86,87] vinyl cyanide (acrylonitrile),[88−90] 1,8-bis(1-propynyl)naphthalene,[91] 1,4-pentadiyne,[79] and malononitrile.[92−94] Similarly, the C═C−C angle of 123.9° is not atypical for carbon substituents on an alkene, when compared to the corresponding angles in vinyl acetylene (123.1°),[86,87] vinyl cyanide (122.2°),[88−90] and propene (124.2°).[95]

Theoretical Calculations. Complete sets of Cartesian coordinates optimized by various theoretical methods are documented in Supporting Information. Along with the present results (which were obtained with SCF, MBPT, and coupled-cluster theories) are three previously published parameter sets that were obtained with density functional theory.[29−31] Of particular interest is the difference between the nominal C═C and C−C distances (δ) predicted by the various levels of theory. Although it is well appreciated that SCF calculations exaggerate bond alternation effects (and therefore predict values of δ that are too large), the accuracy which can be achieved with density functional theory for properties of this sort is not well established. In the present set of results, values obtained for δ in the three DFT-based calculations range from 0.044 to 0.048 Å.

Larger values are found in the coupled-cluster calculations, where δ is approximately a factor of 2 larger than that predicted by DFT. It is notable that both the incorporation of triple excitations in the correlation treatment and expansion of the basis lead to reductions in the value of δ. At the CCSD/TZ2P level, the single bond is predicted to be 0.089 Å longer than the double bond, while inclusion of triple excitations via the CCSD(T) approximation reduces the value of δ to 0.078 Å. Use of the larger cc-pVTZ basis set (238 basis functions) at the CCSD(T) level further reduces δ to 0.073 Å. The structure obtained at the highest level of theory, CCSD(T)/cc-pVTZ, is in excellent agreement with the empirical equilibrium structure derived from a combination of experimental rotational constants and theoretically calculated force fields. In particular, the fully ab initio value of δ obtained at the CCSD(T)/cc-pVTZ level is in perfect agreement with that associated with the empirically determined equilibrium structure. Hence, it seems quite certain that the extent of bond alternation is significantly underestimated by DFT-based methods in this example. For the other distances and angles, CCSD(T)/cc-pVTZ is within 0.002 Å (C≡C triple bond) and 0.4° (C═C−C and C≡C−H) of the experimental values. Given the uncertainty ranges of 0.003 Å and 0.5° ascribed to the latter, the highest-level ab initio results reported here can be said to be in essentially perfect agreement with experiment.

In the past, rotational constants calculated from principal moments of inertia corresponding to CCSD(T)/cc-pVTZ equi-

(85) Ma, B.; Yie, Y.; Schaefer, H. F. *Chem. Phys. Lett.* **1992**, *191*, 521−526.
(86) Fukuyama, T.; Kuchitsu, K.; Morino, Y. *Bull. Chem. Soc. Jpn.* **1969**, *42*, 379−382.
(87) Hirose, C. *Bull. Chem. Soc. Jpn.* **1970**, *43*, 3695−3698.
(88) Costain, C. C.; Stoicheff, B. P. *J. Chem. Phys.* **1959**, *30*, 777−782.
(89) Demaison, J.; Cosleou, J.; Bocquet, R.; Lesarri, A. G. *J. Mol. Spectrosc.* **1994**, *167*, 400−418.
(90) Colmont, J. M.; Wlodarczak, G.; Priem, D.; Muller, H. S. P.; Tien, E. H.; Richards, R. J.; Gerry, M. C. L. *J. Mol. Spectrosc.* **1997**, *181*, 330−344.
(91) Jungk, A. E. *Chem. Ber.* **1972**, *105*, 1595−1613.
(92) Hirota, E.; Morino, Y. *Bull. Chem. Soc. Jpn.* **1960**, *33*, 158−162.
(93) Hirota, E.; Morino, Y. *Bull. Chem. Soc. Jpn.* **1960**, *33*, 705.
(94) Demaison, J.; Wlodarczak, G.; Ruck, H.; Wiedenmann, K. H.; Rudolph, H. D. *J. Mol. Struct.* **1996**, *376*, 399−411.
(95) Le Guennec, M.; Demaison, J.; Wlodarczak, G.; Marsden, C. J. *J. Mol. Spectrosc.* **1993**, *160*, 471−490.

librium structures have proven to be very close to experimental rotational constants, which include vibrational averaging effects. For some other molecules of astrophysical interest—notably several isomers of C_5H_2[96−98] and the related ring-chain compound HC_4N[99]—agreement has been better than 1% for all observed constants. However, this is largely a fortuitous result that arises because of cancellation of errors.[100] Finally, we note that the dipole moment of 0.15 D computed at the CCSD(T)/cc-pVTZ level agrees very well with the value of 0.18 ± 0.01 D determined experimentally.

In passing, it should be noted that the behavior of triple excitation effects on molecular geometries and those associated with expansion of the basis set usually cancel to some extent. In general, triple excitation effects tend to increase internuclear distances while use of larger basis sets leads to reductions. The CCSD level of theory with a basis set similar to TZ2P often gives highly accurate results for structures, as the magnitude of the basis set and triple excitation effects relative to this level of theory tend to be similar. While this behavior can clearly be seen for three of the five bond distances in **1**, the fact that both types of effects lead to reductions in δ is manifested in the atypical behavior of the C═C and C−C distances. As a result, CCSD/TZ2P does not provide a particularly accurate set of equilibrium distances for **1**.

Conclusions

A combined spectroscopic and ab initio approach was used in this study to determine a highly accurate equilibrium structure for *cis*-hex-3-ene-1,5-diyne (**1**). Vibrational corrections to the experimental rotational constants of seven isotopomers of **1** were calculated at several levels of ab initio theory. This has resulted in very accurate equilibrium parameters that confirm a notable shortening of the C−C single bond and lengthening of the C═C double bond from standard values and subtle distortions from nonlinearity in the alkyne units. The distance between terminal carbons of the alkyne moieties (C1−C6 distance) is 4.32 Å. Few highly accurate equilibrium structures are known for molecules containing six or more heavy atoms. This accurate prototype structure can be used to guide future experimental and theoretical work on this and related systems. The spectroscopic data will be useful in searches for radioastronomical evidence for highly unsaturated hydrocarbons in the interstellar medium.

Methods Section

Spectroscopy. The samples used in this project were gaseous solutions of approximately 1% of the enediyne (or its isotopomers) in 99% carrier gas (≈90% neon, 10% helium; used for all isotopomers) at a total pressure between 1.5 and 2.9 atm.

The rotational microwave spectra were recorded with a Balle-Flygare FT microwave spectrometer,[101] operating between 4.5 and 18 GHz, using a General Valve Series 9 pulsed nozzle controlled by a General Valve Iota One pulse controller as the pulsed supersonic nozzle.[102] The FT spectrometer was recently automated on the basis of the design developed at the University of Kiel.[103] The gas expansion axis was perpendicular to the microwave cavity axis, providing average line widths of ≈30 kHz full width at half-maximum. Peak frequencies were reproducible to within 4−5 kHz. Stark effect splittings were observed by applying dc voltages of up to 9.0 kV of opposite polarity to two parallel steel mesh plates (about 30 cm apart).[104] The $J = 1 \leftarrow 0$, transition of OCS was used as a calibration standard (μ(OCS) = 0.71520 D).[105]

Ab Initio Calculations. All calculations reported in this work were performed with a local version of the ACES II program system.[106] Geometry optimizations were performed using the coupled-cluster approximation limited to single and double excitations (CCSD)[107] and CCSD(T), in which CCSD is augmented by a correction for triple excitation effects.[108] Analytical gradient methods[109,110] were used to determine the equilibrium geometries and corresponding dipole moments. Basis sets used in the geometry optimizations were a triple-ζ plus double-polarization (TZ2P) basis[111] and the correlation consistent cc-pVTZ basis of Dunning.[112]

In addition, the quadratic and cubic force fields of **1** were determined at the self-consistent field level of theory by a procedure based on numerical differentiation of analytically computed second derivatives.[75,113,114] These were then used to calculate vibrational corrections to the rotational constants according to the formulas described by Mills.[115] A (nearly negligible) correction for centrifugal distortion effects needed to convert rotational constants belonging to the set of Watson's determinable parameters to equilibrium rotational constants was calculated on the basis of the equations given by Kirchhoff.[116]

General Synthetic Methods. Benzene and CH_2Cl_2 were freshly distilled from CaH_2. THF was first distilled from CaH_2, followed by distillation from Na/benzophenone. Acetonitrile was stirred over K_2CO_3 for 24 h, stirred over P_2O_5 for 24 h, and then distilled onto 4-Å molecular sieves. *n*-Butylamine was stirred over CaH_2 overnight and then distilled onto 4-Å sieves. $Ba^{13}CO_3$ was purchased from Cambridge Isotope Laboratories. All other compounds were purchased from commercial sources and used without further purification. Photolyses utilized a Hanovia 450-W medium-pressure Hg lamp. ^{1}H and ^{13}C NMR spectra (Bruker AC-300 spectrometer) and ^{2}H NMR spectra (Bruker

(96) Seburg, R. A.; McMahon, R. J.; Stanton, J. F.; Gauss, J. *J. Am. Chem. Soc.* **1997**, *119*, 10838−10845.
(97) Travers, M. J.; McCarthy, M. C.; Gottlieb, C. A.; Thaddeus, P. *Astrophys. J.* **1997**, *483*, L135−L138.
(98) Gottlieb, C. A.; McCarthy, M. C.; Gordon, V. D.; Chakan, J. M.; Apponi, A. J.; Thaddeus, P. *Astrophys. J.* **1998**, *509*, L141−L144.
(99) McCarthy, M. C.; Grabow, J. U.; Travers, M. J.; Chen, W.; Gottlieb, C. A.; Thaddeus, P. *Astrophys. J.* **1999**, *513*, 305−310.
(100) At the CCSD(T)/cc-pVTZ level of theory, the treatment of electron correlation is often nearly quantitative, and basis set insufficiency is the largest source of error. Hence, bond lengths tend to be somewhat too long and rotational constants somewhat smaller than those of the exact equilibrium structure. When the magnitude of this error is comparable to that of vibrational averaging (which also tends to make B_0 constants smaller than the corresponding B_e values), agreement between calculated B_e values and experimental B_0 constants can be excellent. B_e constants calculated from the CCSD(T)/cc-pVTZ structure in the present case (7053, 2580, and 1889 MHz), however, are in less satisfactory agreement with the experimental B_0^S values; errors are +1.4%, −1.6%, and −0.6%, respectively. This is due almost entirely to the relatively poor prediction of the C═C−C bond angle. When the bond angle is changed from 124.3° to 123.9° and the rest of the CCSD(T)/cc-pVTZ structural parameters are not modified, differences between the corresponding B_e constants and the experimental B_0^S values are reduced by an order of magnitude.

(101) Balle, T. J.; Flygare, W. H. *Rev. Sci. Instrum.* **1981**, *52*, 33−45.
(102) Hillig, K. W.; Matos, J.; Scioly, A.; Kuczkowski, R. L. *Chem. Phys. Lett.* **1987**, *133*, 359−362.
(103) Grabow, J.-U. Ph.D. Thesis, University of Kiel: 1992.
(104) Bohn, R. K.; Hillig, K. W.; Kuczkowski, R. L. *J. Phys. Chem.* **1989**, *93*, 3456−3459.
(105) Tanaka, K.; Ito, H.; Harada, K.; Tanaka, T. *J. Chem. Phys.* **1984**, *80*, 5893−5905.
(106) Stanton, J. F.; Gauss, J.; Watts, J. D.; Lauderdale, W. J.; Bartlett, R. J. *Int. J. Quantum Chem.* **1992**, *S26*, 879−894.
(107) Purvis, G. D.; Bartlett, R. J. *J. Chem. Phys.* **1982**, *76*, 1910−1918.
(108) Raghavachari, K.; Trucks, G. W.; Pople, J. A.; Head-Gordon, M. *Chem. Phys. Lett.* **1989**, *157*, 479−483.
(109) Scheiner, A. C.; Scuseria, G. E.; Rice, J. E.; Lee, T. J.; Schaefer, H. F. *J. Chem. Phys.* **1987**, *87*, 5361−5373.
(110) Watts, J. D.; Gauss, J.; Bartlett, R. J. *Chem. Phys. Lett.* **1992**, *200*, 1−7.
(111) Szalay, P. G.; Stanton, J. F.; Bartlett, R. J. *Chem. Phys. Lett.* **1992**, *193*, 573−577.
(112) Dunning, T. H. *J. Chem. Phys.* **1989**, *90*, 1007−1023.
(113) Gauss, J.; Stanton, J. F. *Chem. Phys. Lett.* **1997**, *276*, 70−77.
(114) Schneider, W.; Thiel, W. *Chem. Phys. Lett.* **1989**, *157*, 367−373.
(115) Mills, I. M. Vibration−Rotation Structure in Asymmetric- and Symmetric-Top Molecules. In *Molecular Spectroscopy: Modern Research*; Rao, K. N., Mathews, C. W., Eds.; Academic Press: New York, 1972; Vol. 1, pp 115−140.
(116) Kirchhoff, W. H. *J. Mol. Spectrosc.* **1972**, *41*, 333−380.

AM-500 spectrometer) were obtained in $CDCl_3$ or $CHCl_3$, respectively, with chemical shifts referenced to the residual solvent. All air- or moisture-sensitive reactions were carried out under a nitrogen atmosphere under anhydrous conditions. Flash column chromatography was conducted on silica gel (EM Science 60, 230−400 mesh).

Sample Preparation and Handling. Enediyne samples were prepared by tetra-*n*-butylammonium fluoride-mediated deprotection of a bis-trimethylsilyl protected precursor using a two-phase reaction in ethylene glycol, H_2O, or D_2O. Vacuum distillation (1.0 Torr, 1 h, room temperature) of the crude reaction mixture afforded the deprotected enediyne, along with minor impurities, in a liquid-nitrogen-cooled flask. The deprotected enediyne was thawed, transferred to a dry glass ampule via syringe, cooled in liquid nitrogen, and sealed under vacuum. In the case of the deuterated samples, the ampules were prewashed with D_2O to minimize loss of deuterium at the acetylenic position via isotopic exchange with the glass surface. Ampules were packaged in a Styrofoam container in dry ice and shipped to the University of Michigan for characterization by Fourier transform microwave spectroscopy. ^{1}H NMR spectroscopy of these samples often revealed Me_3SiF, Et_2O, D_2O, and H_2O as impurities, but these impurities did not interfere with accurate measurement of rotational spectra.

***cis*-1,6-Bis(trimethylsilyl)hex-3-ene-1,5-diyne (5).**[64] A flask charged with $Pd(PPh_3)_4$ (0.867 g, 0.75 mmol) and CuI (0.286 g, 1.5 mmol) was subjected to 3 pump/$Ar_{(g)}$ flush cycles. *n*-Butylamine (6.8 mL, 68.8 mmol) and *cis*-1,2-dichloroethylene (1.13 mL, 15.0 mmol) were then added. A solution of (trimethylsilyl)acetylene (4.86 mL, 34.4 mmol) in benzene (25 mL) was added over 5 h via a syringe pump and the reaction stirred under Ar for an additional 9 h. The reaction was quenched with saturated aqueous NH_4Cl (25 mL), and extracted with Et_2O (3 × 25 mL). The combined organic layers were washed with brine (25 mL), dried over $MgSO_4$, filtered, and the solvent removed by rotary evaporation to yield a thick brown oil. A pentane/ether solution (1:1; 10 mL) was added and the precipitate that formed was removed by filtration. The pentane/ether was removed by rotary evaporation and the resulting brown oil purified by flash column chromatography (SiO_2, 5% CH_2Cl_2 in hexanes, $R_f = 0.40$) to yield 2.71 g (12.3 mmol, 82%) of enediyne **5** as a yellow oil: ^{1}H NMR δ 0.20 (s, 18 H), 5.84 (s, 2 H).

***cis*-Hex-3-ene-1,5-diyne (1).** In the distillation pot of a short-path distillation apparatus, tetra-*n*-butylammonium fluoride trihydrate (6.58 g, 20.9 mmol) was dissolved in ethylene glycol (10 mL). To this stirred solution, enediyne **5** (2.10 g, 9.53 mmol) was added dropwise and stirred for 3 h at room temperature. High boiling impurities were removed via vacuum distillation (15 Torr, 30 min, room temperature). Enediyne **1**, along with minor impurities, was then collected directly from the reaction mixture via vacuum distillation (1.0 Torr, 1 h, room temperature) into a liquid-nitrogen-cooled flask. Two layers were normally seen after collection was complete. The bottom, aqueous layer was removed with a pipet to yield a clear oil: ^{1}H NMR δ 3.37 (s, 2 H), 5.89 (s, 2 H).

[1-^{2}H]- and [1,6-^{2}H]-*cis*-Hex-3-ene-1,5-diyne ([1-^{2}H]-1 and [1,6-^{2}H]-1). Tetra-*n*-butylammonium fluoride was prepared in the following manner: Tetra-*n*-butylammonium fluoride trihydrate (14.20 g, 45.0 mmol) was heated to 45−47 °C at 0.02 Torr for 72 h. This "anhydrous" Bu_4NF[117] was rehydrated with D_2O (7 mL) and subsequently subjected to dehydration at 45−47 °C at 0.02 Torr with three additions of D_2O (7 mL) in 12−15-h intervals, with no dehydration after the last addition. Enediyne **5** (3.3 g, 15.0 mmol) was added dropwise to this stirred solution of Bu_4NF/D_2O and allowed to stir for 3 h at room temperature. Vacuum distillation (1.0 Torr, room temperature) directly from the reaction mixture yielded [1-^{2}H]-**1** and [1,6-^{2}H]-**1** as a clear liquid: ^{1}H NMR δ 5.87 (s). ^{2}H NMR δ 3.4 (s).

[3-^{2}H]- and [3,4-^{2}H]-*cis*-Hex-3-ene-1,5-diyne ([3-^{2}H]-1 and [3,4-^{2}H]-1). Tetra-*n*-butylammonium fluoride (14.20 g, 45.0 mmol) was prepared as described for [1,6-^{2}H]-**1**. Enediyne **5** (3.3 g, 15.0 mmol) was added dropwise to a stirred solution of Bu_4NF/D_2O and allowed to stir for 3 h at room temperature. Vacuum distillation of the product (1.0 Torr, room temperature) directly from the reaction mixture and through a pyrolysis tube heated to 270 °C yielded a mixture of [1-^{2}H]-**1**, [3-^{2}H]-**1**, [1,6-^{2}H]-**1**, and [3,4-^{2}H]-**1**: ^{2}H NMR δ 3.4 (s, 1.0 D), 5.9 (s, 0.44 D).

3-Trimethylsilyl-[1-^{13}C]-propynoic Acid. A 100-mL round-bottom flask, equipped with a sidearm attached to a N_2/vacuum manifold, was charged with $Ba^{13}CO_3$ (6.75 g, 34.0 mmol) and fitted with an addition funnel charged with concentrated H_2SO_4 (50 mL, 938 mmol). This addition funnel was fitted with another addition funnel filled with Drierite, which was attached to a three-neck 250-mL round-bottom flask via thick-walled rubber tubing. The 250-mL round-bottom flask was also attached to a N_2/vacuum manifold. The entire system was evacuated to 1.0 Torr and a static vacuum held. The 250-mL round-bottom flask was cooled in liquid N_2 and H_2SO_4 slowly dripped onto the $Ba^{13}CO_3$. The liberated $^{13}CO_2$ was collected in the liquid-N_2-cooled flask. In a separate flask, (trimethylsilyl)acetylene (4.7 mL, 33.3 mmol) was added to THF (100 mL) and cooled to −78 °C. *n*-BuLi (13.2 mL, 2.5 M in hexane) was added via syringe and the solution stirred for 45 min. The solution of acetylide anion was then frozen on top of the $^{13}CO_2$ via cannula transfer, the liquid-N_2 bath replaced with a −78 °C bath, and the solution allowed to stir for 1 h. EtOH (35 mL) was added, followed by HCl (42 mL, 1 M) and the solution allowed to warm to room temperature. Et_2O (50 mL) was added and the layers were separated. The aqueous layer was extracted with Et_2O (3 × 50 mL), and the organic layers were combined, washed with brine (50 mL) and water (50 mL), dried over $MgSO_4$, and filtered. Solvent was reduced by rotary evaporation to give the carboxylic acid in a concentrated ether solution: ^{1}H NMR δ 0.23 (s, 9 H), 6.4 (bs, 1 H). ^{13}C NMR δ 155.2.

Methyl 3-trimethylsilyl-[1-^{13}C]-propynoate. This reaction employed the Diazald apparatus (Aldrich). Diazald (7.23 g, 33.7 mmol) dissolved in Et_2O (45 mL) was slowly dripped into a solution of KOH (11.23 g, 200 mmol) in EtOH (20 mL) and H_2O (17 mL) heated to 60 °C. The resulting vapor of diazomethane and diethyl ether condensed on the coldfinger (−78 °C) and dripped directly into a stirred solution of 3-trimethylsilyl-[1-^{13}C]-propynoic acid (33 mmol) in Et_2O (25 mL) cooled to 0 °C (ice bath). After Diazald addition was complete, the solvent was removed via rotary evaporation, yielding a yellow oil. The oil was purified by vacuum distillation (87 °C, 12 mmHg) to yield 2.27 g (43% in two steps) of the ester as a clear oil: ^{1}H NMR δ 0.23 (s, 9 H), 3.75 (d, $J[^{13}C-^1H] = 4.5$ Hz, 3 H). ^{13}C NMR δ 153.3 (q, $J[^{13}C-^1H] = 4.5$ Hz).

3-Trimethylsilyl-[1-^{13}C]-propynal. DIBAL-H (30 mL, 1.0 M in hexane) was added dropwise over 30 min to a solution of methyl 3-trimethylsilyl-[1-^{13}C]-propynoate (2.27 g, 17.8 mmol) dissolved in CH_2Cl_2 (90 mL) at −78 °C. After addition was complete, the reaction was stirred at −78 °C for 1 h and quenched by the addition of MeOH (20 mL), followed by HCl (35 mL, 1 M), and allowed to warm to room temperature. H_2SO_4 (1 M) was added until the solution was clear. The layers were separated and the aqueous layer was extracted with CH_2Cl_2 (3 × 50 mL). The organic layers were combined, washed with saturated aqueous $NaHCO_3$ (50 mL), brine (50 mL), and H_2O (50 mL), and dried over $MgSO_4$. The solvent was removed by rotary evaporation to yield 1.71 g (76%) of the aldehyde as a clear oil: ^{1}H NMR δ 0.24 (s, 9 H), 9.14 (d, $J[^{13}C-^1H] = 192.6$ Hz, 1 H). ^{13}C NMR δ 176.8 (d, $J[^{13}C-^1H] = 192.8$ Hz).

1,6-Bis(trimethylsilyl)-[3-^{13}C]-hex-3-ene-1,5-diyne ([3-^{13}C]-5). *n*-BuLi (4.5 mL, 2.5 M in hexane) was added to a stirred suspension of triphenyl-(3-trimethylsilylprop-2-ynl)phosphonium bromide[118] (5.26 g, 11.6 mmol) in THF (100 mL) at −78 °C and the resulting dark red solution was stirred for 15 min. In a separate flask, 3-trimethylsilyl-[1-^{13}C]-propynal (1.45 g, 11.4 mmol) was dissolved in THF (100 mL) and cooled to −78 °C. The solution of the aldehyde was added to the preformed ylide via cannula and stirred for 1.75 h at −78 °C. The reaction was quenched with saturated aqueous NH_4Cl (50 mL), followed

(117) Cox, P. D.; Terpinski, J.; Lawrynowicz, W. J. *J. Org. Chem.* **1984**, *49*, 3216−3219.

(118) Hann, M. M.; Sammes, P. G.; Kennewell, P. D.; Taylor, J. B. *J. Chem. Soc., Perkin Trans. 1* **1982**, 307−314.

(119) Harmony, M. D.; Laurie, V. W.; Kuczkowski, R. L.; Schwendeman, R. H.; Ramsey, D. A.; Lovas, F. J.; Lafferty, W. J.; Maki, A. G. *J. Phys. Chem. Ref. Data* **1979**, *8*, 619−721.

(120) Berry, R. J.; Harmony, M. D. *Struct. Chem.* **1989**, *1*, 49−59.

(121) Tam, H. S.; Choe, J.-I.; Harmony, M. D. *J. Phys. Chem.* **1991**, *95*, 9267−9272.

by H_2O (50 mL), and allowed to warm to room temperature. The layers were separated and the aqueous layer extracted with Et_2O (3 × 50 mL). The organic layers were combined, washed with brine (50 mL), dried over $MgSO_4$, and filtered. The solvent was removed by rotary evaporation to yield a black tar. The tar was purified by flash column chromatography (SiO_2, hexanes) to yield 0.21 g of the trans isomer as a white solid and 0.23 g of the cis isomer as a yellow oil, with an overall yield of 17.5%. The yield of the cis isomer could be increased by photoisomerization of the trans isomer in MeCN (3 h, quartz filter) to a 3:2 mixture of cis and trans isomers. Trans isomer: ^{1}H NMR δ 0.18 (s, 18 H), 5.98 (dd, $J[^{13}C-^1H]$ = 168.0 Hz, J = 16.1 Hz, 1H), 5.98 (dd, $J[^{13}C-^1H]$ = 5.9 Hz, J = 16.1 Hz, 1 H). ^{13}C NMR δ 121.7 (dd, $J[^{13}C-^1H]$ = 168.0, 5.8 Hz), R_f = 0.60. Cis isomer: ^{1}H NMR δ 0.21 (s, 18 H), 5.84 (dd, $J[^{13}C-^1H]$ = 168.9 Hz, J = 11.1 Hz, 1 H), 5.84 (dd, $J[^{13}C-^1H]$ = 2.7 Hz, J = 11.1 Hz, 1 H). ^{13}C NMR δ 120.6 (dd, $J[^{13}C-^1H]$ = 168.6, 2.7 Hz), R_f = 0.46.

[3-^{13}C]-*cis*-Hex-3-ene-1,5-diyne ([3-^{13}C]-1). Labeled enediyne **[**3-^{13}C]-**5** (0.25 g) was mixed with unlabeled enediyne **5** (2.17 g) to provide a sample with approximately 10% isotopic enrichment. Deprotection and isolation were performed in the manner described for unlabeled enediyne **1**.

Acknowledgment. The authors gratefully acknowledge funding support from the National Science Foundation (CHE-9800716, R.J.M.; CHE-9527359, R.L.K.; CHE-9873818, J.F.S.; Graduate Fellowship, R.L.F.) and the Robert A. Welch Foundation (J.F.S.).

Supporting Information Available: Tables of rotational transition frequencies for all isotopomers; Cartesian coordinates, harmonic vibrational frequencies, and infrared intensities computed at SCF/DZP, SDQ-MBPT(4)/DZP, and SDQ-MBPT(4)/TZ2P. Optimized Cartesian coordinates obtained at CCSD(T)/cc-pVTZ. This material is available free of charge via the Internet at http://pubs.acs.org.

JA9934908